JOURNAL OF CHEMICAL INFORMATION AND MODELING

Article

pubs.acs.org/jcim

MMGBSA As a Tool To Understand the Binding Affinities of Filamin–Peptide Interactions

Mikko Ylilauri and Olli T. Pentikäinen*

Computational Bioscience Laboratory, Department of Biological and Environmental Science & Nanoscience Center, University of Jyväskylä, P.O. Box 35, Jyväskylä FI-40014, Finland

Supporting Information

ABSTRACT: Filamins (FLN) are large dimeric proteins that cross-link actin and work as important scaffolds in human cells. FLNs consist of an N-terminal actin-binding domain followed by 24 immunoglobulin-like domains (FLN1–24). FLN domains are divided into four subgroups based on their amino acid sequences. One of these subgroups, including domains 4, 9, 12, 17, 19, 21, and 23, shares a similar ligand-binding site between the β strands C and D. Several proteins, such as integrins β2 and β7, glycoprotein Ibα (GPIbα), and migfilin, have been shown to bind to this site. Here, we computationally estimated the binding free energies of filamin A (FLNa) subunits with bound peptides using the molecular mechanics-generalized Born surface area (MMGBSA) method. The obtained computational results correlated well with the experimental data, and they ranked efficiently both the binding of one ligand to all used FLNa-domains and the binding of all used ligands to FLNa21. Furthermore, the steered molecular dynamics (SMD) simulations pinpointed the binding hot spots for these complexes. These results demonstrate that molecular dynamics combined with free energy calculations are applicable to estimating the energetics of protein–protein interactions and can be used to direct the development of novel FLN function modulators.

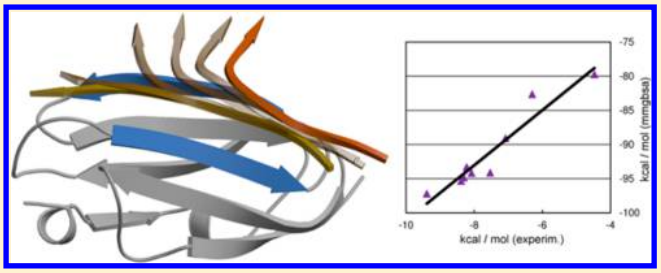

INTRODUCTION

Filamin A (FLNa) is part of an extensively studied family of proteins that work as versatile tools in cells. FLNs are able to bind and stabilize the three-dimensional F-actin network. This so-called actin cytoskeleton plays a crucial role in the locomotion and mechanical resistance of the cell. In addition to actin, FLN has a vast number of binding partners that are linked to many important cellular activities, such as signaling pathways and cell migration;[1,2] thus, it is a potential target in the research of novel cancer treatments.[3] The structure of all FLN isoforms (A, B, and C) is similar: an actin-binding domain at the N-terminal end is followed by FLN-domains 1–24.[4] As the FLN24 dimerizes, the functional full-length protein is an extended homodimer with two 280 kDa polypeptide chains.[5] Each monomer is further divided into two rods that are separated by a flexible hinge region: rod 1 consists of domains 1–15, and rod 2 consists of domains 16–23.[4,6] Another hinge separates rod 2 from the C-terminal dimerization domain (FLN24).[7] Rod 2 is an interesting target for protein–protein interaction studies because it does not bind F-actin and thus is able to communicate with partner proteins. Indeed, rod 2 domains are known to bind many partners,[2] many of which are GTP-binding proteins or proteins related to cytoskeleton or cell adhesion.

All rod 2 domains of FLNa fold similarly: they have approximately 90 to 100 amino acids that fold into compact structures of β-plated sheets. In all known FLNa structures with a binding partner, the binding site for the ligand–peptide is a groove formed between β strands C and D of the FLN-domain (e.g., see refs 8–10). The binding peptide is positioned at the groove as an additional β strand, with mostly hydrophobic residues facing the CD-face. It is also known that the rod 2 has a more compact structure than the rod 1 has, in which even-numbered domains pair tightly with an adjacent odd-numbered domain.[2] In the case of domain pairs 18–19 and 20–21, the A strand of the even domain binds the CD-face of the adjacent odd domain, masking its ligand-binding site and supposedly working as an autoinhibitor in these domains.[11,12]

According to a previous bioinformational analysis,[13] FLN-domains can be divided to distinct subgroups. One of these subgroups, the so-called group A, contains all the odd-numbered domains of rod 2 (FLN17, 19, 21, and 23) and also domains FLN4, 9, and 12 from rod 1. These domains are grouped together because they share a conserved CD-face capable of binding similar peptides. Indeed, it has been shown that many binding-partners of FLN can associate with more than one domain; for example, migfilin, a cytoskeletal adaptor protein disconnecting FLNa from integrin, is known to bind to several rod 2 domains.[9,14] The study of FLN-domain division[13] also showed in experimental methods that all the domains

Received: April 26, 2013
Published: August 29, 2013

ACS Publications © 2013 American Chemical Society

dx.doi.org/10.1021/ci4002475 | J. Chem. Inf. Model. 2013, 53, 2626–2633

belonging to group A bind integrin β2 and β7 cytoplasmic tails, migfilin, and glycoprotein Ibα (GPIbα).

Previously, protein−protein or protein−peptide binding, in the context of FLN, was studied in several experimental methods, including steady-state measurement by spectrophotometer,[15] solid-phase binding assay with radiolabeled ligands,[16] affinity chromatography pull-down assay,[9,17] isothermal titration calorimetry (ITC),[13] and single-molecule mechanical measurements.[18] Computational methods have recently emerged as a fast and inexpensive approach to study protein−ligand and protein−protein interaction.[19] For example, the molecular dynamics (MD) simulation-based molecular mechanics/generalized Born surface area (MMGBSA) method has been successfully utilized not only to predict the free energy of binding between protein and small molecule ligands[20−22] but also to study many protein−peptide and protein−protein complexes.[23,24] In MMGBSA, the free energy of binding is calculated by using a combination of gas phase energy (MM), electrostatic solvation energy (GB), and nonelectrostatic contribution to solvation energy (SA). Typically, the free energy of binding is estimated as an average of several protein and ligand complex conformations obtained from MD simulation trajectories.[25,26] It must be noted that it is also possible to calculate the MMGBSA-values from static entities, such as structures solved with X-ray crystallography. However, the usage of MD simulations has several advantages: (1) MD simulations of the complex can predict relatively large conformational changes of both binding partners as well as different kinds of interactions between them;[27−29] (2) the structures obtained with X-ray crystallography can show uncertainties in the placement of amino acid side chains into the electron density;[30,31] and (3) if the complex is formed with computational techniques, the starting conformation does not necessarily describe the energetically most favorable complex structure, as in the several cases investigated in this study.

In this study, we show that by using MMGBSA calculations, the computational prediction correlates well with the experimentally measured binding affinities of peptides to FLNa-domains. For example, our calculations are in excellent agreement with previous ITC experiments for the binding of GPIbα to FLNa group A domains.[13] Furthermore, as an example of this computational approach to binding estimations, we studied FLNa related biological problems using the MMGBSA method. In addition to interactions involving β-sheets, this computational approach is suitable for calculating other protein−protein interactions, and it could ease the estimation of binding affinities of already existing or newly made peptides aimed at interacting with pharmacologically important protein targets.

METHODS

Protein Structures. The atomic coordinates for FLNa21 (PDB: 2BRQ,[10] chain A) and FLNa17 (PDB: 2BP3[8]) were retrieved from the correspondent crystal structures. For the remaining FLNa domains studied (4, 9, 12, 19, and 23), homology models were built based on the alignment of the crystal structure of FLNa21 with bound integrin β tail (PDB: 2BRQ) and the corresponding subsection of the human FLNa sequence (Uniprot: FLNA_HUMAN). This was done either because there were no crystal or NMR structures available for FLNa9 and 12 or because the folding of the CD-face would be disunited if the correspondent structures available on the PDB-database were used. All the homology models were made using MALIGN in BODIL[32] and NEST.[33] The FLNa starting structures were superimposed using VERTAA in BODIL. The stereochemical quality of the models was verified with Ramachandran plots obtained by PROCHECK[34] (Supporting Information Figure S1).

Peptide Structures. Structures for the peptides were retrieved from the crystal structure complexes with FLNa domains. Peptides used in the study were integrin cytoplasmic tail peptides β2 (from PDB: 2JF1[35]) and β7 (from PDB: 2BRQ), migfilin (from PDB: 2W0P[9]), and GBIbα (from PDB: 2BP3). The peptides were superimposed to attain the same binding conformation for each FLNa−peptide complex as in the migfilin-FLNa21 crystal structure. To obtain comparable MMGBSA results with all peptide-ligands, their length was unified and set to 11 residues. With migfilin, this required adding two residues to the structure of peptide obtained from the FLNa−migfilin complex (PDB: 2W0P). This was done by homology modeling from an alignment of the migfilin sequence (Uniprot: FBLI1_HUMAN) and the structure of integrin β7 bound FLNa21 (PDB: 2BRQ).

MD Simulations. The energy minimization and MD simulations were carried out with NAMD2.6[36] utilizing Amber ff03 force field parameters. Hydrogen atoms were added with TLEAP in Antechamber-1.27,[37] and the system was solvated with a rectangular box of transferable intermolecular potential three-point (TIP3P) water molecules extending 13 Å in every direction around the solute. The equilibration of the system was performed as follows. First, the energy minimization of the water molecules, counterions, and amino acid side-chains (1,500 steps) was performed, while the rest of the system was kept constrained by restraining Cα atoms with a harmonic force of 5 kcal/mol/Å^2. In the second step, the whole system was energy minimized without constrains (500 steps) followed by an MD simulation run with restrained Cα atoms in constant pressure (180,000 steps). Finally, unstrained production MD simulations of 6 ns were performed. All production simulations were repeated three times. The temperature was kept at 300 K with Langevin dynamics for all non-hydrogen atoms using a Langevin damping coefficient of 5 ps^{-1}. The pressure was kept at 1 atm with Nosé-Hoover Langevin piston[38] with an oscillation time scale of 200 fs and a damping time scale of 100 fs. An integration time step of 2 fs was used under a multiple time stepping scheme.[39] The bonded and short-range interactions were calculated every step and long range electrostatic interactions every third step. A cutoff value of 12 Å was used for the short-range electrostatic interactions and van der Waals forces, and a switching function was enforced for the van der Waals forces to smoothen the cutoff. The simulations were conducted under periodic boundary conditions, and the long-range electrostatics were counted with the particle mesh Ewald method.[40] The hydrogen bonds were restrained by the SHAKE algorithm.[41]

SMD Simulations. In steered molecular dynamics (SMD) simulations, the Cα atoms of FLNa domain were kept fixed, while an external force was applied to the center of mass of the Cα atoms of the peptide. The direction of the constant force (ranging from 100 to 200 pN) was defined by the vector that links the center of mass of Cα atoms of FLNa and the binding partner. The SMD simulations were performed as with constraint-free runs, except that the production simulations of 2.4 ns were performed only after 720 ps unrestrained MD simulation. The time step used in SMD production runs was 1 fs.

dx.doi.org/10.1021/ci4002475 | J. Chem. Inf. Model. 2013, 53, 2626−2633

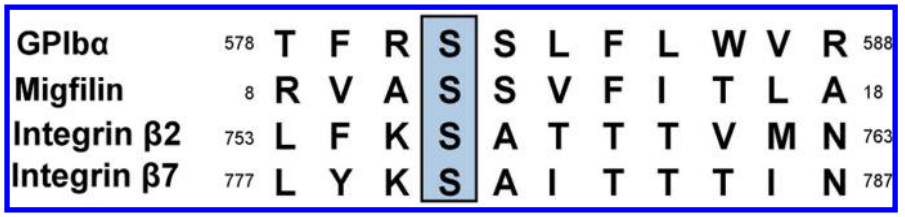

Figure 1. Structure-based sequence alignment of the peptide-ligands used in the study. The serine in position 4, which is capable of bonding with a residue from D strand of FLNa, is highlighted in a blue box.

Table 1. Free Energies for the Binding of GPIbα to FLNa Domains, Calculated by MMGBSA[b]

method	FLNa9	FLNa12	FLNa17	FLNa19	FLNa21	FLNa23
comp. (igb = 1)	−94.2 ± 1.1	−89.1 ± 2.6	−95.3 ± 2.1	−93.3 ± 2.6	−97.2 ± 0 0.8	−94.8 ± 1.5
comp. (igb = 2)	−74.6 ± 0.7	−68.9 ± 2.2	−73.8 ± 2.5	−72.5 ± 2.2	−76.9 ± 1.5	−72.6 ± 0.4
comp. (igb = 5)	−63.6 ± 5.3	−50.1 ± 5.0	−58.9 ± 8.1	−55.3 ± 9.9	−60.0 ± 3.8	−55.9 ± 6.9
exptl[a]	−8.08	−7.08	−8.38	−8.22	−9.39	−8.31

[a]Experimental K_d values obtained from ref 13 and converted to ΔG_{bind}. [b]Estimations of ΔG_{bind} (in kcal/mol) are based on snapshots obtained from trajectories after 6 ns-MD simulations. The average of three repeats, and the standard errors, is shown for each complex and for each GB-model tested. In addition, the experimental values, which were obtained from the literature and utilized for calculating the correlation coefficients, are shown for each complex. Results of each individual repeat are shown in Supporting Information Table S1.

Trajectory Analysis. Trajectory analyses of MD and SMD simulations were done by extracting snapshots at 1.2 and 0.6 ps intervals (respectively) with PTRAJ in ANTECHAMBER 1.27.[37] Visual inspection of snapshots was performed with BODIL. A cutoff value of 3.4 Å was used as the upper limit for a hydrogen bonding distance.

MMGBSA. The free energies for the binding of ligands (ΔG_{bind} in kcal/mol) were calculated from the MD trajectories using the MMGBSA method[25,26] implemented in Amber10.[42] For each FLN−peptide complex, the binding free energy of MMGBSA was estimated as follows: $\Delta G_{bind} = G_{complex} - G_{protein} - G_{ligand}$ where ΔG_{bind} is the binding free energy and $G_{complex}$, $G_{protein}$, and G_{ligand} are the free energies of complex, protein, and ligand, respectively. The energies were estimated according to the equation $\Delta E_{MM} + \Delta G_{GB} + \Delta G_{nonpolar} - T\Delta S$ where ΔE_{MM} is the gas-phase interaction energy between FLN and a binding peptide, including the electrostatic and the van der Waals energies; ΔG_{GB} and $\Delta G_{nonpolar}$ are the polar and nonpolar components of the desolvation free energy, respectively; $T\Delta S$ is the change of conformational entropy on ligand binding, which was not considered here as it has been found that the calculations of entropic contribution are often neither reasonable nor necessary when ranking binding affinities of similar ligands.[23,43] E_{MM} was determined with the Sander program from Amber with infinite cutoff, and $G_{nonpolar}$ was estimated from the solvent accessible surface area using Molsurf.[44] G_{GB} was calculated with the GB approach implemented in Amber. Dielectric constants of 1 and 80 were used for solute and solvent, respectively. The parameters for GB-calculations developed by Tsui and Case (igb = 1;[25]) or Onufriev et al. (igb = 2 (α = 0.8, β = 0.0, γ = 2.909); igb = 5 (α = 1.0, β = 0.8, γ = 4.85)[45]) were used. Binding free energy values were calculated from snapshots taken from the MD complex trajectory at 6 ps intervals from the whole 6 ns-MD simulation.

Figures. Figures were generated with BODIL v. 0.81 and MOLSCRIPT v. 2.1.2[46] and rendered with RASTER3D v. 2.7C.[47]

RESULTS AND DISCUSSION

MMGBSA Calculations of Peptide-Ligand Bound FLNa-Domains. A recent experimental study[13] showed that GPIbα binds to FLNa group A domains in the micromolar range, with FLNa21 showing the highest affinity. According to these results obtained with ITC, it is possible to rank domains according to their binding affinities. Additionally, in the same study, GPIbα was noted to have higher affinity to FLNa21 when compared to migfilin or integrin β2 or β7 cytoplasmic tails. Because FLNa is a pharmacologically interesting target, it is desirable to design and build short peptides and peptide mimetics capable of binding to the CD-face of FLN-domains. Using computational calculations is the fastest and the most cost-effective way to make estimates of changes in binding affinity. Furthermore, when MD-based MMGBSA calculations are utilized for that purpose, the dynamic nature of the protein−peptide interaction can be taken into account. In this study, we calculated the binding affinities of FLNa-domains that share a similar binding groove between C and D strands to various short peptides (Figure 1). The exact conformation of the peptides bound to the groove and the residues that take part in the event are known from the corresponding crystal structures. In addition, the modeled FLNa−peptide complexes used in our study, when superimposed with the template structure, showed highly similar conformations. Consequently, we were able to make a plausible assumption of the binding conformation of all the studied peptides to be used in MD simulations and MMGBSA calculations. The results of these calculations were then compared to those reported earlier using experimental methods.

First, the binding affinities of GPIbα to FLNa4, 9, 12, 17, 19, 21, and 23 were calculated. After a 6 ns nonconstrained MD simulation, snapshots were extracted from the trajectory, and ΔG_{bind} was calculated from them for the whole simulation. The average ΔG for each FLNa21−peptide complex was calculated based on three repeats. Because there are currently no experimental results available for FLNa4 bound GPIbα, it was omitted from the comparison. This exclusion was also relevant because the conformation of the FLNc4 CD-face, as noticed in the recently solved crystal structure (PDB: 3V8O, *submitted work*), differs from that of the other group A member domains.

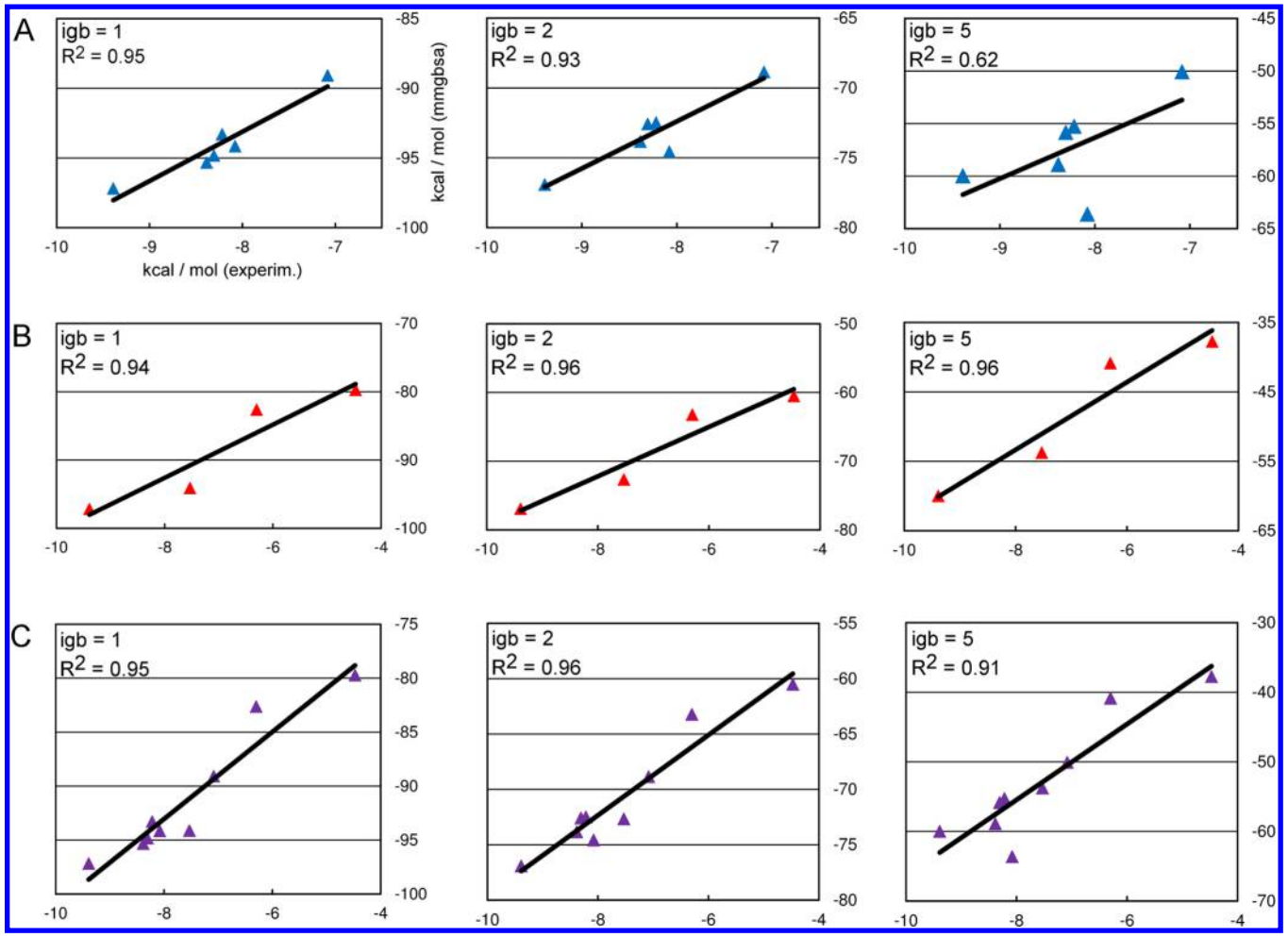

Figure 2. The correlation coefficient (R^2) between experimental results and computational estimations of binding affinities of filamin–ligand complexes. Experimental results are taken from a recent study,[13] and computational estimations were obtained using MMGBSA. (A) GPIbα bound to FLNa domains 9, 12, 17, 19, 21, and 23. (B) FLNa domain 21 in complex with GPIbα, migfilin, integrin β2, or integrin β7. (C) Combined results from plots shown in (A) and (B). The correlation coefficients and the GB-model used are marked in each chart. Numerical results are shown in Tables 1 and 2 and in Supporting Information Tables S1 and S2.

Table 2. Free Energies for the Binding of Various Ligands to FLNa21, Calculated by MMGBSA[b]

method	GPIbα	migfilin	integrin β2	integrin β7
comp. (igb = 1)	−97.2 ± 0.8	−94.1 ± 4.8	−79.7 ± 0.6	−82.6 ± 2.9
comp. (igb = 2)	−76.9 ± 1.5	−72.7 ± 3.9	−60.5 ± 0.7	−63.2 ± 1.9
comp. (igb = 5)	−60.0 ± 3.8	−53.8 ± 6.9	−37.8 ± 1.7	−40.9 ± 4.6
exptl[a]	−9.39	−7.53	−4.47	−6.30

[a]Experimental K_d values obtained from ref 13 and converted to ΔG_{bind}. [b]Estimations of ΔG_{bind} (in kcal/mol) are based on snapshots obtained from trajectories after 6 ns-MD simulations. The average of three repeats, with the standard errors, is shown for each complex and for each GB-model tested. In addition, the experimental values, which were obtained from the literature and utilized for calculating the correlation coefficients, are shown for each complex. Results of each individual repeat are shown in Supporting Information Table S2.

Consequently, in our MD simulations the GPIbα repetitiously disengaged from the CD-face, precluding the MMGBSA calculations.

The results obtained in various FLNa domains with bound GPIbα were compared to recently reported experimental values (Table 1 and Figure 2A). It is noticeable that the correlation coefficient (R^2) between experimental results and our computational estimation was as high as 0.95. In addition to the model generated by Tsui and Case,[25] two other GB-models (igb = 2 and igb = 5, generated by Onufriev et al.[45]) were also tested. With the first of these models (igb = 2), the correlation was high (R^2 = 0.93). As for the other model (igb = 5), the correlation coefficient was only moderate (R^2 = 0.62). This is likely due to a relatively large fluctuation of the energy level with this GB-model, which is seen in the standard deviations of the runs (Table 1 and Supporting Information Table S1). The large variation is visible also when the binding free energies from individual runs are plotted against simulation time (Supporting Information Figure S2): with igb = 5, the energy level fluctuates more than with the other two GB-models. In most cases, the free energies calculated from individual repeats have converged well. However, due to the nature of MD-based MMGBSA, this does not occur invariably. Indeed, it has been shown in a recent study that it is impossible to equilibrate

dx.doi.org/10.1021/ci4002475 | J. Chem. Inf. Model. 2013, 53, 2626−2633

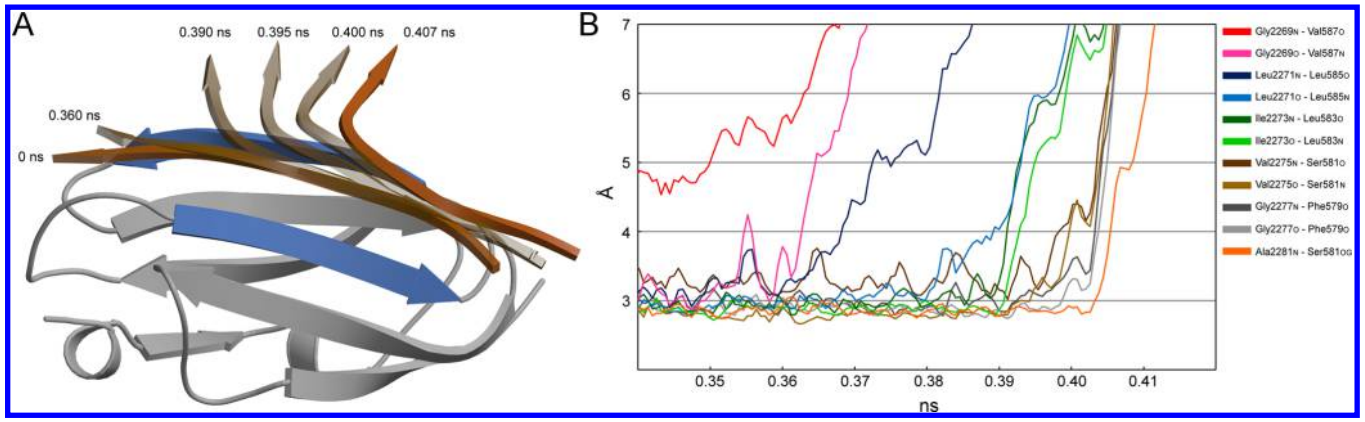

Figure 3. SMD simulations show the release of the bound peptide from the CD-face. In (A), a view of FLNa21 CD-face (blue) with bound GPIbα (orange) is shown. In addition to the starting structure, where the GPIbα is firmly bound to the binding groove, snapshots taken from the SMD simulation trajectory are also shown. The snapshots show that the N-terminal of the peptide is the last to disengage in the course of simulation, where the ligand is pulled and the FLN is kept fixed. The chart in (B) shows the atom distances (moving averages, period of 3) between atoms from the D-face of FLNa21 and GPIbα. In addition to the main chain N or O atoms, the side-chain O(H) of serine in position 4 of the ligand (Ser581) is considered. As the chart shows, the hydrogen bond between the side chain of the serine and an atom from the C strand of FLN is the last to come loose in the SMD simulation. Atom distances from the SMD simulations between FLNa21 and the remaining studied ligands are shown in Supporting Information Figure S3.

proteins in MD simulations.[48] Consequently, it has been suggested that it is more efficient to calculate MMGBSA energies on averages from several short simulations than from a single long run.[48,49] Therefore, the average of three MD simulation repeats calculated in this study gives a good estimate of the binding free energy for each filamin–ligand complex.

In summary, it can be deduced that the molecular dynamics together with the MMGBSA calculations are in good agreement with experimental studies, especially with the first two GB-models mentioned above. However, since with igb = 5 the correlation is lower than with other models, and the standard deviations are clearly larger, perhaps the GB-models 1 and 2 would be preferable choices for the evaluation of binding affinities in this type of studies.

Next, the ΔG_{bind} for various peptide-ligands binding to FLNa21 was estimated. It was reported earlier that GPIbα shows a higher affinity toward FLNa21 than migfilin or integrin β2 and β7 cytoplasmic tails.[13,18] This was also clearly seen in our results with the MMGBSA method (Table 2 and Figure 2B). The correlation to experimental results was very high (R^2 = 0.94, R^2 = 0.96 and R^2 = 0.96 for igb = 1, igb = 2, and igb = 5, respectively). However, it is important to note that the results were based on only four different ligands, so the feasibility of correlation is somewhat doubtful. Nevertheless, with the above-mentioned good correlation results between GPIbα and different FLNa domains, the results of various peptides binding to FLNa21 clearly pinpoint that the MD-based computational method for estimating binding affinities is comparable to the experimental methods. Indeed, when all the results are combined and placed in the same plot, the correlation is at a very good level regardless of the GB-model used (Figure 2C). This shows that calculations based on homology models respond well to those obtained with crystal structures. Because the correlations shown in Figure 2C were good with all GB-models, only igb = 1 was applied in the remaining MMGBSA calculations.

SMD Simulations of FLN–Peptide Interaction. In SMD simulations, the Cα atoms of FLN domains were fixed, while a constant external force was applied to the center of mass of the Cα atoms of the bound peptide. These simulations enabled the atom-level analysis of the interaction between FLN and the binding partner peptides. It also helped to reveal the hot spots, that is, the residues of the peptide, which are crucial to the adherence to the FLN binding groove. It was reported recently by mechanical single-molecule measurement that compared to migfilin or integrin β7, GPIbα shows a stronger affinity to FLN.[18] This was also seen in our 2.4 ns SMD simulations: Whereas β2 regularly disengaged from FLNa21 with a 150 pN and even with a 100 pN force, the GPIbα required a force as high as 200 pN in order to detach. However, the forces used in our study are not comparable to the much lower forces used in the above-mentioned study, which used mechanical single-molecule measurements, because of the differences in the way the force was applied.

It is interesting to note that the disengagement of the peptide in the SMD simulations always started from the C-terminal even though the external force was applied evenly to all Cα atoms of the bound peptide (Figure 3A). This was also clearly seen in the atom distances between the main chain N and O atoms in the FLN C-strand and bound peptide (Figure 3B and Supporting Information Figure S3). Measured from the SMD trajectories, these distances represent the hydrogen bonds existing between the FLN main chain atoms and the bound peptide. In addition to the hydrogen bonds between the FLN C strand and the peptide, all peptides used in this study exhibited a serine in position 4 capable of bonding with a residue from D strand of FLN (Figure 1). This obviously strengthened the affinity of the peptide. Indeed, the distance measurements indicate that this particular hydrogen bond between FLN and the side-chain of serine of the bound peptide was the last bond to break when force was applied (Figure 3B and Supporting Information Figure S3).

It is important to note that although applying a force evenly to all Cα atoms of the peptide highlights the crucial interactions between FLN and peptide, this equal distribution of the force may not be the case in biological contexts. It is also possible that the bound peptide *in vivo* disengages differently than observed in our simulations. Indeed, in a recent study in which SMD was utilized to study autoinhibition of FLNa21 by A strand from FLNa20,[50] the disengaging was noted to start from

dx.doi.org/10.1021/ci4002475 | J. Chem. Inf. Model. 2013, 53, 2626–2633

the N-terminal. However, a direct comparison of our results with that study is not reasonable because the setup was different. Unlike the single domains used in our study, in the previous study a three-domain complex of FLN domains 19−21 was used, and force was applied only to the N-terminus of FLNa19 while C-terminus of FLNa21 was kept fixed. In the above-mentioned study, which used singe-molecule measurements,[18] the force was also directed to the N-terminus of the bound ligand. As our SMD calculations suggested, the interactions close to this terminus are much harder to break, so the release of the peptide *in vivo* would likely occur rapidly, unlike in our simulations where the release was more gradual. The force needed to release the bound peptide would also be much higher if it was applied only to the N-terminus. This was noticed in our simulations when the FLN domain was kept fixed, and only the Cα of the first residue in the peptide was pulled; the force needed to release the bound peptide was in the nN-range, that is, it was significantly higher than when the force was applied to the whole peptide.

Autoinhibition of FLNa21. Next, we studied FLN related biological problems with MD-based computational methods. One such problem, recently experimentally studied, is the masking, or autoinhibition, of FLNa21 by the A-strand from the adjacent FLNa20.[11,51] We calculated the free energy of binding of the A-strand from FLNa20 in complex with FLNa21 CD-face. The result (average of three repeats) of the whole 6 ns-MD simulation showed that ΔG_{bind} for this binding event was −82.7 kcal/mol. Accordingly, the binding affinity of the A strand of FLNa20 to FLNa21 was at a level similar to integrin β2 and β7 cytoplasmic tails (−79.7 kcal/mol and −82.6 kcal/mol, respectively; Table 2). However, both migfilin and GPIbα had a clearly higher binding affinity to FLNa21 compared to the A-strand of FLNa20 (−94.1 kcal/mol and −97.2 kcal/mol, respectively; Table 2). These results suggest that at least migfilin and GPIbα are able to relieve the autoinhibition of the FLNa21 binding site. This phenomenon was previously presented in migfilin, using nuclear magnetic resonance spectroscopy.[52] However, contrary to previous suggestions based on spectroscopy analysis,[13] integrin β tail might not be able to replace efficiently the autoinhibition of FLNa21, at least when the FLN is not already in a mechanically strained conformation.

The Binding Mode of Migfilin to FLNa21. A study reporting the crystal structure of FLNa21 in complex with migfilin showed that a single migfilin peptide is able to bind two FLNa21 domains.[9] However, based on solution state NMR experiments, it was suggested that only one of the interactions (chain A) seen in the crystal is biologically relevant. According to the authors, it would however still be possible that, under certain contexts, migfilin might engage two FLNa domains simultaneously.[9] To confirm this possibility, we calculated the free energy of binding of migfilin with the chain B of FLNa21, which was taken from the corresponding crystal structure (PDB: 2W0P). The MMGBSA results from 6 ns-MD simulation snapshots showed that the ΔG_{bind} for binding of migfilin to FLNa21 chain B was −70.9 kcal/mol, which corresponded to an experimental value of −2.4 kcal/mol, based on the equation of the correlation curve shown in Figure 2B. This result is significantly worse than the result using the FLNa21 chain A (−94.1 kcal/mol; Table 2) or any other domain studied. The result suggests that the engagement of two FLNs by a single migfilin peptide is an unlikely event *in vivo*, regardless of whether the FLN is mechanically stressed or not. The migfilin might be able to connect temporarily, for example, the two monomers from the same FLN homodimer, but the affinity is too weak for this conformation to persist.

CONCLUSIONS

We estimated the binding free energies of filamin A subunits with bound peptides using an *in silico* MMGBSA method. Our computational results correlated well with the experimental data and were able to rank reliably both the binding of one ligand to all used FLNa-domains and the binding of all used ligands to FLNa21. Furthermore, we showed that the correlation was at a high level independent of the GB-model used. In the steered molecular dynamics simulations, we were able to indicate the crucial parts of the FLNa−peptide interaction at the binding groove. These results demonstrate that molecular dynamics based methods are capable of both estimating the energetics of protein−protein interactions and analyzing the atom-level events that occur. Thus, these methods can be used to direct the development of novel FLN function modulators.

ASSOCIATED CONTENT

Supporting Information

Three additional figures (Figures S1−S3) and two supporting tables (Table S1 and Table S2). This material is available free of charge via the Internet at http://pubs.acs.org.

AUTHOR INFORMATION

Corresponding Author

*Phone: +358405216913. E-mail: olli.t.pentikainen@jyu.fi. Corresponding author address: Survontie 9, Nanoscience Center, University of Jyväskylä, Jyväskylä FI-40014, Finland.

Notes

The authors declare no competing financial interest.

ACKNOWLEDGMENTS

This study was funded by the National Doctoral Programme in Informational and Structural Biology (M.Y.). CSC - The Finnish IT Centre for Science is acknowledged for their generous computational grants (O.T.P. projects jyy2516 and jyy2586).

ABBREVIATION:

FLN, filamin; FLNa, filamin A; GPIbα, glycoprotein Ibα; ITC, isothermal titration calorimetry; MD, molecular dynamics; MMGBSA, molecular mechanics-generalized Born surface area; SMD, steered molecular dynamics

REFERENCES

(1) Zhou, A.; Hartwig, J. H.; Akyürek, L. M. Filamins in cell signaling, transcription and organ development. *Trends Cell Biol.* **2010**, *20*, 113−123.

(2) Nakamura, F.; Stossel, T. P.; Hartwig, J. H. The filamins: organizers of cell structure and function. *Cell Adh. Migr.* **2011**, *5*, 160−169.

(3) Jiang, X.; Yue, J.; Lu, H.; Campbell, N.; Yang, Q.; Lan, S.; Haffty, B. G.; Yuang, C.; Shen, Z. Inhibition of filamin-a reduces cancer metastatic potential. *Int. J. Biol. Sci.* **2013**, *9*, 67−77.

(4) van der Flier, A.; Sonnenberg, A. Structural and functional aspects of filamins. *Biochim. Biophys. Acta* **2001**, *1538*, 99−117.

(5) Gorlin, J. B.; Yamin, R.; Egan, S.; Stewart, M.; Stossel, T. P.; Kwiatkowski, D. J.; Hartwig, J. H. Human endothelial actin-binding

protein (abp-280, nonmuscle filamin): a molecular leaf spring. *J. Cell Biol.* **1990**, *111*, 1089−1105.
(6) Stossel, T. P.; Condeelis, J.; Cooley, L.; Hartwig, J. H.; Noegel, A.; Schleicher, M.; Shapiro, S. S. Filamins as integrators of cell mechanics and signalling. *Nat. Rev. Mol. Cell Biol.* **2001**, *2*, 138−145.
(7) Pudas, R.; Kiema, T.; Butler, P. J. G.; Stewart, M.; Ylänne, J. Structural basis for vertebrate filamin dimerization. *Structure* **2005**, *13*, 111−119.
(8) Nakamura, F.; Pudas, R.; Heikkinen, O.; Permi, P.; Kilpeläinen, I.; Munday, A. D.; Hartwig, J. H.; Stossel, T. P.; Ylänne, J. The structure of the gpib-filamin a complex. *Blood* **2006**, *107*, 1925−1932.
(9) Lad, Y.; Jiang, P.; Ruskamo, S.; Harburger, D. S.; Ylänne, J.; Campbell, I. D.; Calderwood, D. A. Structural basis of the migfilin-filamin interaction and competition with integrin beta tails. *J. Biol. Chem.* **2008**, *283*, 35154−35163.
(10) Kiema, T.; Lad, Y.; Jiang, P.; Oxley, C. L.; Baldassarre, M.; Wegener, K. L.; Campbell, I. D.; Ylänne, J.; Calderwood, D. A. The molecular basis of filamin binding to integrins and competition with talin. *Mol. Cell* **2006**, *21*, 337−347.
(11) Lad, Y.; Kiema, T.; Jiang, P.; Pentikäinen, O. T.; Coles, C. H.; Campbell, I. D.; Calderwood, D. A.; Ylänne, J. Structure of three tandem filamin domains reveals auto-inhibition of ligand binding. *EMBO J.* **2007**, *26*, 3993−4004.
(12) Heikkinen, O. K.; Ruskamo, S.; Konarev, P. V.; Svergun, D.; Iivanainen, T.; Heikkinen, S. M.; Permi, P.; Koskela, H.; Kilpeläinen, I.; Ylänne, J. Atomic structures of two novel immunoglobulin-like domain pairs in the actin cross-linking protein filamin. *J. Biol. Chem.* **2009**, *284*, 25450−25458.
(13) Ithychanda, S. S.; Hsu, D.; Li, H.; Yan, L.; Liu, D. D.; Das, M.; Plow, E. F.; Qin, J. Identification and characterization of multiple similar ligand-binding repeats in filamin: implication on filamin-mediated receptor clustering and cross-talk. *J. Biol. Chem.* **2009**, *284*, 35113−35121.
(14) Ithychanda, S. S.; Das, M.; Ma, Y.; Ding, K.; Wang, X.; Gupta, S.; Wu, C.; Plow, E. F.; Qin, J. Migfilin, a molecular switch in regulation of integrin activation. *J. Biol. Chem.* **2009**, *284*, 4713−4722.
(15) Goldmann, W. H. Kinetic determination of focal adhesion protein formation. *Biochem. Biophys. Res. Commun.* **2000**, *271*, 553−557.
(16) Sharma, C. P.; Ezzell, R. M.; Arnaout, M. A. Direct interaction of filamin (abp-280) with the beta 2-integrin subunit cd18. *J. Immunol.* **1995**, *154*, 3461−3470.
(17) Travis, M. A.; van der Flier, A.; Kammerer, R. A.; Mould, A. P.; Sonnenberg, A.; Humphries, M. J. Interaction of filamin a with the integrin beta 7 cytoplasmic domain: role of alternative splicing and phosphorylation. *FEBS Lett.* **2004**, *569*, 185−190.
(18) Rognoni, L.; Stigler, J.; Pelz, B.; Ylänne, J.; Rief, M. Dynamic force sensing of filamin revealed in single-molecule experiments. *Proc. Natl. Acad. Sci. U. S. A.* **2012**, *109*, 19679−19684.
(19) Massova, I.; Kollman, P. Computational alanine scanning to probe protein−protein interactions: a novel approach to evaluate binding free energies. *J. Am. Chem. Soc.* **1999**, *121*, 8133−8143.
(20) Rastelli, G.; Del Rio, A.; Degliesposti, G.; Sgobba, M. Fast and accurate predictions of binding free energies using mm-pbsa and mm-gbsa. *J. Comput. Chem.* **2010**, *31*, 797−810.
(21) Niinivehmas, S. P.; Virtanen, S. I.; Lehtonen, J. V.; Postila, P. A.; Pentikäinen, O. T. Comparison of virtual high-throughput screening methods for the identification of phosphodiesterase-5 inhibitors. *J. Chem. Inf. Model.* **2011**, *51*, 1353−1363.
(22) Hou, T.; Wang, J.; Li, Y.; Wang, W. Assessing the performance of the mm/pbsa and mm/gbsa methods. 1. the accuracy of binding free energy calculations based on molecular dynamics simulations. *J. Chem. Inf. Model.* **2011**, *51*, 69−82.
(23) Gohlke, H.; Case, D. A. Converging free energy estimates: mm-pb(gb)sa studies on the protein-protein complex ras-raf. *J. Comput. Chem.* **2004**, *25*, 238−250.
(24) Zuo, Z.; Gandhi, N. S.; Arndt, K. M.; Mancera, R. L. Free energy calculations of the interactions of c-jun-based synthetic peptides with the c-fos protein. *Biopolymers* **2012**, *97*, 899−909.
(25) Tsui, V.; Case, D. A. Theory and applications of the generalized born solvation model in macromolecular simulations. *Biopolymers* **2000−2001**, *56*, 275−291.
(26) Kollman, P. A.; Massova, I.; Reyes, C.; Kuhn, B.; Huo, S.; Chong, L.; Lee, M.; Lee, T.; Duan, Y.; Wang, W.; Donini, O.; Cieplak, P.; Srinivasan, J.; Case, D. A.; Cheatham, T. E. 3. Calculating structures and free energies of complex molecules: combining molecular mechanics and continuum models. *Acc. Chem. Res.* **2000**, *33*, 889−897.
(27) Ylilauri, M.; Pentikäinen, O. T. Structural mechanism of n-methyl-d-aspartate receptor type 1 partial agonism. *PLoS One* **2012**, *7*, e47604.
(28) Postila, P. A.; Ylilauri, M.; Pentikäinen, O. T. Full and partial agonism of ionotropic glutamate receptors indicated by molecular dynamics simulations. *J. Chem. Inf. Model.* **2011**, *51*, 1037−1047.
(29) Postila, P. A.; Swanson, G. T.; Pentikäinen, O. T. Exploring kainate receptor pharmacology using molecular dynamics simulations. *Neuropharmacology* **2010**, *58*, 515−527.
(30) Joosten, R. P.; Joosten, K.; Cohen, S. X.; Vriend, G.; Perrakis, A. Automatic rebuilding and optimization of crystallographic structures in the protein data bank. *Bioinformatics* **2011**, *27*, 3392−3398.
(31) Cooper, D. R.; Porebski, P. J.; Chruszcz, M.; Minor, W. X-ray crystallography: assessment and validation of protein-small molecule complexes for drug discovery. *Expert Opin. Drug. Discovery* **2011**, *6*, 771−782.
(32) Lehtonen, J. V.; Still, D.; Rantanen, V.; Ekholm, J.; Björklund, D.; Iftikhar, Z.; Huhtala, M.; Repo, S.; Jussila, A.; Jaakkola, J.; Pentikäinen, O.; Nyrönen, T.; Salminen, T.; Gyllenberg, M.; Johnson, M. S. Bodil: a molecular modeling environment for structure-function analysis and drug design. *J. Comput.-Aided Mol. Des.* **2004**, *18*, 401−419.
(33) Petrey, D.; Xiang, Z.; Tang, C. L.; Xie, L.; Gimpelev, M.; Mitros, T.; Soto, C. S.; Goldsmith-Fischman, S.; Kernytsky, A.; Schlessinger, A.; Koh, I. Y. Y.; Alexov, E.; Honig, B. Using multiple structure alignments, fast model building, and energetic analysis in fold recognition and homology modeling. *Proteins* **2003**, *53* (Suppl 6), 430−435.
(34) Laskowski, R. A.; MacArthur, M. W.; Moss, D. S.; Thornton, J. M. Procheck: a program to check the stereochemical quality of protein structures. *J. Appl. Crystallogr.* **1993**, *26*, 283−291.
(35) Takala, H.; Nurminen, E.; Nurmi, S. M.; Aatonen, M.; Strandin, T.; Takatalo, M.; Kiema, T.; Gahmberg, C. G.; Ylänne, J.; Fagerholm, S. C. Beta2 integrin phosphorylation on thr758 acts as a molecular switch to regulate 14-3-3 and filamin binding. *Blood* **2008**, *112*, 1853−1862.
(36) Phillips, J. C.; Braun, R.; Wang, W.; Gumbart, J.; Tajkhorshid, E.; Villa, E.; Chipot, C.; Skeel, R. D.; Kalé, L.; Schulten, K. Scalable molecular dynamics with namd. *J. Comput. Chem.* **2005**, *26*, 1781−1802.
(37) Wang, H.; Liu, Y.; Huai, Q.; Cai, J.; Zoraghi, R.; Francis, S. H.; Corbin, J. D.; Robinson, H.; Xin, Z.; Lin, G.; Ke, H. Multiple conformations of phosphodiesterase-5: implications for enzyme function and drug development. *J. Biol. Chem.* **2006**, *281*, 21469−21479.
(38) Feller, S. E.; Zhang, Y.; Pastor, R. W. Constant pressure molecular dynamics simulation: the langevin piston method. *J. Chem. Phys.* **1995**, *103*, 4613−4621.
(39) Schlick, T.; Skeel, R. D.; Brunger, A. T.; Kalé, L. V.; Board, J. A. J.; Hermans, J.; Schulten, K. Algorithmic challenges in computational molecular biophysics. *J. Comput. Phys.* **1999**, *151*, 9−48.
(40) Darden, T.; York, D.; Pedersen, L. Particle mesh Ewald: an w log(n) method for ewald sums in large systems. *J. Chem. Phys.* **1993**, *98*, 10089−10092.
(41) Ryckaert, J.; Ciccotti, G.; Berendsen, H. J. Numerical integration of the cartesian equations of motion of a system with constraints: molecular dynamics of n-alkanes. *J. Comput. Phys.* **1977**, *23*, 327.
(42) Case, D. A.; Cheatham, T. E., III; Darden, T.; Gohlke, H.; Luo, R.; Merz, K. M. J.; Onufriev, A.; Simmerling, C.; Wang, B.; Woods, R. J. The amber biomolecular simulation programs. *J. Comput. Chem.* **2005**, *26*, 1668−1688.

(43) Hou, T.; Chen, K.; McLaughlin, W. A.; Lu, B.; Wang, W. Computational analysis and prediction of the binding motif and protein interacting partners of the abl sh3 domain. *PLoS Comput. Biol.* **2006**, *2*, e1.
(44) Connolly, M. L. Analytical molecular surface calculation. *J. Appl. Crystallogr.* **1983**, *16*, 548−558.
(45) Onufriev, A.; Bashford, D.; Case, D. A. Exploring protein native states and large-scale conformational changes with a modified generalized born model. *Proteins* **2004**, *55*, 383−394.
(46) Kraulis, P. Molscript: a program to produce both detailed and schematic plots of protein structures. *J. Appl. Crystallogr.* **1991**, *24*, 946−950.
(47) Merritt, E. A.; Bacon, D. J. Raster3d: photorealistic molecular graphics. *Methods Enzymol.* **1997**, *277*, 505−524.
(48) Genheden, S.; Ryde, U. Will molecular dynamics simulations of proteins ever reach equilibrium? *Phys. Chem. Chem. Phys.* **2012**, *14*, 8662−8677.
(49) Genheden, S.; Ryde, U. How to obtain statistically converged mm/gbsa results. *J. Comput. Chem.* **2010**, *31*, 837−846.
(50) Pentikäinen, U.; Ylänne, J. The regulation mechanism for the auto-inhibition of binding of human filamin a to integrin. *J. Mol. Biol.* **2009**, *393*, 644−657.
(51) Heikkinen, O. K.; Ruskamo, S.; Konarev, P. V.; Svergun, D. I.; Iivanainen, T.; Heikkinen, S. M.; Permi, P.; Koskela, H.; Kilpeläinen, I.; Ylänne, J. Atomic structures of two novel immunoglobulin-like domain pairs in the actin cross-linking protein filamin. *J. Biol. Chem.* **2009**, *284*, 25450−25458.
(52) Ithychanda, S. S.; Qin, J. Evidence for multisite ligand binding and stretching of filamin by integrin and migfilin. *Biochemistry* **2011**, *50*, 4229−4231.